Submitted to The Astronomical Journal

High resolution infrared spectra of Bulge Globular Clusters: The extreme chemical abundances of Terzan 4 and Terzan 5

Livia Origlia

Osservatorio Astronomico di Bologna, Via Ranzani 1, I–40127 Bologna, Italy

origlia@bo.astro.it

R. Michael Rich

Math-Sciences 8979, Department of Physics and Astronomy, University of California at Los Angeles, Los Angeles, CA 90095-1562

rmr@astro.ucla.edu

ABSTRACT

Using the NIRSPEC spectrograph at Keck II, we have obtained infrared echelle spectra covering the range $1.5 - 1.8$ μm for the highly reddened bulge globular clusters Terzan 4 and Terzan 5. The clusters are of interest because a blue horizontal branch in Terzan 4 is consistent with very low metallicity, while Terzan 5 has been proposed as possibly the most metal rich known Galactic globular cluster. We report the first detailed abundance analysis for stars in these clusters, and we find [Fe/H]=–1.60 and –0.21 dex for Terzan 4 and Terzan 5, respectively, confirming the presence of a large metallicity spread in the bulge as well as in the halo of the Galaxy. We find [α/Fe] $\approx$ +0.5 dex in Terzan 4 and [α/Fe] $\approx$ +0.3 dex in Terzan 5, consistent with what has been found for field stars in the bulge. The enhanced $\alpha-$element abundances are also consistent with rapid chemical enrichment, most likely by type II SNe. Finally, we measure very low $^{12}C/^{13}C\leq$ 10 ratios in all the giant stars, confirming that extra-mixing mechanisms due to *cool bottom processing* occur during evolution along the RGB.

Subject headings: Galaxy: bulge, globular clusters: individual (Terzan 4 and Terzan 5) — stars: abundances, late–type — techniques: spectroscopic

[1]Data presented herein were obtained at the W.M.Keck Observatory, which is operated as a scientific partnership among the California Institute of Technology, the University of California, and the National Aeronautics and Space Administration. The Observatory was made possible by the generous financial support of the W.M. Keck Foundation.

1. Introduction

The detailed study of the abundance patterns of iron-peak, CNO and α elements in field and globular cluster stellar populations is a fundamental step required to understand the star formation and chemical evolution history of our Galaxy. These elements are synthesized in stars of different masses, hence on different timescales and play a crucial role in disentangling evolutionary mixing effects from primordial enrichment (Wheeler, Sneden & Truran 1989, McWilliam 1997)

Globular clusters represent the best astrophysical templates for the study of the early Galactic evolution since they are the oldest objects and their age is well constrained, allowing a reliable calibration of a possible age–metallicity relation (McWilliam 1997), a fundamental constraint for any chemical evolution model. In addition, they are equally present in the halo, the thick disk and the bulge of our Galaxy (see e.g. Armandroff 1989, Minniti 1995), therefore they represent unique chemical fossils to trace the early epoch of the Galaxy formation.

Reliable elemental abundances are now available for field stars (see e.g. Boesgaard et al. 1999; Gratton et al. 2000, Carretta, Gratton & Sneden 2000 and reference therein) while are still very incomplete for globular clusters. In halo/disk field stars the average [α/Fe] abundance ratio shows a general enhancement of 0.3–0.5 dex with respect to the Solar value up to [Fe/H]$\approx$–1 and a linear decreasing trend towards Solar [α/Fe] with further increasing metallicity. The actual position of the knee (i.e. the metallicity at which [α/Fe] begins to decrease) depends on the type Ia SN timescales and it is also a function of the Star Formation (SF) rate, while the amount of α enhancement depends on the initial mass function of the progenitors of the type II SNe (see McWilliam 1997).

While the classic halo globular clusters have a mean [α/Fe]$\approx$+0.4, too few measurements have been done at the high metallicity end to define the trend there (e.g. Kraft 1994, Carney 1996). Bulge globular clusters are ideal targets to study the behavior of the abundance patterns in the high metallicity domain, but foreground extinction is so great as to largely preclude optical studies of any kind, particularly at high spectral resolution.

The most accurate abundance determinations in the Galactic bulge obtained so far and based on high resolution optical spectroscopy refer to a sample of K giants in Baade's window (McWilliam & Rich 1994, hereafter MWR94; Rich & McWilliam 2000) and a few giants in two globular clusters, NGC 6553 and NGC 6528 (Barbuy et al. 1999; Cohen et al. 1999; Carretta et al. 2001).

With the availability of NIRSPEC, a high throughput infrared (IR) echelle spectrograph at the Keck Observatory (McLean et al. 1998), came the prospect of measuring the composition of the clusters in the bulge. Recently, we observed two bright giants in Liller 1 and NGC 6553 with NIRSPEC and our abundance analysis has been presented in Origlia, Rich & Castro (2002, hereafter ORC02). We find [Fe/H] $= -0.3 \pm 0.2$ and [O/Fe] $= +0.3 \pm 0.1$ We also measure strong lines for the other $\alpha-$elements Mg, Ca, and Si, obtaining an overall [α/Fe] $= +0.3 \pm 0.2$ dex.

In this paper we present the high resolution IR observations and the abundance analysis for a sample of bright giants in two additional globular clusters, namely Terzan 4 and Terzan 5. These

clusters are of special interest because they span the entire abundance range present in the bulge. These clusters suffer from large foreground extinction (E(B–V)≥2), precluding any optical study at high spectral resolution. Recent HST–NICMOS photometry (Ortolani et al. 2001) suggests old ages for these clusters and confirms previous photometric estimates for their metallicities (Ortolani, Barbuy & Bica 1996, 1997): roughly Solar for Terzan 5 and as low as 1/100 Solar for Terzan 4. Ortolani et al. (1997) argue that a blue horizontal branch is present in Terzan 4, however the small numbers of stars in their color-magnitude diagram (CMD) requires an independent metallicity measurement in order for the case to be more convincing. More recent NICMOS photometry of Terzan 5 (Cohn et al. 2002) confirms the presence of an old turnoff point and a CMD consistent with high metallicity. The recent photometry confirms that both clusters lie within ~ 1 kpc of the Galactic center.

Our observations and data reduction follow in Sect. 2. Sect. 3 discusses our abundance analysis and in Sect. 4 the resulting metallicities and radial velocities are presented. Our concluding remarks are given in Sect. 5.

2. Observations and Data Reduction

Near infrared, high-resolution echelle spectra of four bright giants in the cores of the bulge globular clusters Terzan 4 and Terzan 5 have been acquired on 23 June 2001 and 15 July 2002. We used the infrared spectrograph NIRSPEC (McLean et al. 1998) which is at the Nasmyth focus of the Keck II telescope. The high resolution echelle mode, with a slit width of $0\farcs43$ (3 pixels) and a length of $24''$ and the standard NIRSPEC-5 setting, which covers most of the 1.5–1.8 micron H-band, have been selected. Typical exposure times (on source) ranged from 4 to 16 minutes. Fig. 1 shows the H band images of the observed core region of Terzan 4 and Terzan 5 taken with the slit viewing camera (SCAM) of NIRSPEC, which has a field of view of $46''\times46''$ and a scale of $0\farcs183\ pixel^{-1}$.

The raw spectra of the observed stars have been reduced using the REDSPEC IDL-based package written at the UCLA IR Laboratory. Each order has been sky subtracted by using nodding pairs and flat-field corrected. Wavelength calibration has been performed using arc lamps and a second order polynomial solution, while telluric features have been removed by dividing by the featureless spectrum of an O star. At the NIRSPEC resolution of R=25,000 several single roto-vibrational OH lines and CO bandheads can be measured to derive accurate oxygen and carbon abundances. Other metal abundances can be derived from the atomic lines of Fe I, Mg I, Si I, Ti I and Ca I. Abundance analysis is performed by using full spectral synthesis techniques and equivalent width measurements of representative lines.

3. Abundance Analysis

We compute suitable synthetic spectra of giant stars by varying the stellar parameters and the element abundances using an updated version of the code described in Origlia, Moorwood & Oliva (1993) (see also ORC02). The code uses the LTE approximation and is based on the molecular blanketed model atmospheres of Johnson, Bernat & Krupp (1980) which have been extensively used for abundance studies based on high resolution spectra of cool stars (e.g. Lambert et al. 1984, Smith & Lambert 1985, 1990). For temperatures above 4000 K the code uses the ATLAS9 models. Since in the IR the major source of continuum opacity is H^- with its minimum near 1.6 μm, the dependence of the results on the choice of model atmospheres is much less critical than in the visual range.

Three main compilations of atomic oscillator strengths are used: the Kurucz database (c.f. *http://cfa-www.harward.edu/amdata/ampdata/kurucz23/sekur.html*), Bièmont & Grevesse (1973) and Meléndez & Barbuy (1999, hereafter MB99). On average, MB99 log-gf values are systematically lower than Kurucz ones but in most cases the difference does not exceed 0.2 dex and the overall scatter in the derived abundances is < 0.1 dex (see ORC02 for a more quantitative comparison). The molecular oscillator strengths and excitation potentials have been computed as described in Origlia et al. (1993). The dissociation energies of the molecules are from Table 2 in Johnson et al. (1980), the reference Solar abundances from Grevesse & Sauval (1998).

Photometric estimates of the stellar parameters are initially used as input to produce a grid of model spectra, allowing the abundances and abundance patterns to vary over a large range and the stellar parameters around the photometric values. The model which better reproduces the overall observed spectrum and the line equivalent widths of selected lines is targetted as the best-fit model. We measure equivalent widths in the observed spectrum, and in the best fit model and for four models which are, respectively, 0.1 and 0.2 dex away from the best fit. This approach gives us the uncertainties listed in Table 2.

Uncertainties in the stellar parameters of $\pm$200 K in temperature (T_{eff}), $\pm$0.5 dex in log-gravity (log g) and $\pm$0.5 km s^{-1} in microturbulence velocity (ξ), can introduce a further systematic $\leq$0.2 dex uncertainty in the absolute abundances. However, since the CO and OH molecular line profiles are very sensitive to effective temperature, gravity, and microturbulence variations, they constrain better the values of these parameters, significantly reducing their initial range of variation and ensuring a good self-consistency of the overall spectral synthesis procedure (see ORC02). Solutions with $\Delta T_{eff} = \pm 200$ K, Δlog g$=\pm 0.5$ dex and $\Delta\xi = \mp 0.5$ km s^{-1} and corresponding $\pm$0.2 dex abundance variations from the best-fit one are indeed less statistically significant (typically at $1 \leq \sigma \leq 3$ level only, see Sect. 4). Moreover, since the stellar features under consideration show a similar trend with variations in the stellar parameters, although with different sensitivities, *relative* abundances are less dependent on stellar parameter assumptions and their values can be well constrained down to $\approx \pm 0.1$ dex.

4. Results

By combining full spectral synthesis analysis with equivalent width measurements we derive accurate abundances of Fe, C, O and [O/Fe] and $^{12}C/^{13}C$ abundance patterns for the four observed giants in Terzan 4 and Terzan 5. The abundances of other $\alpha-$elements, Ca, Si, Mg and Ti, are obtained by measuring a few strong neutral lines. These lines are generally heavily saturated and are consequently somewhat less sensitive to abundance variations than the molecular CO and OH lines, which give a very accurate C and O abundances (see ORC02).

From the NIRSPEC spectra we also derived their heliocentric radial velocities with a ± 5 km s^{-1} uncertainty. Average values of -50 ± 3 km/s with a dispersion $\sigma \pm 5.5$ km/s in Terzan 4 and of -93 ± 2 km/s with a dispersion $\sigma \pm 3.6$ km/s in Terzan 5 have been obtained. The inferred radial velocities are fully consistent with those listed by Harris (1996;1999), namely –53 and –94 km s^{-1} for Terzan 4 and Terzan 5, respectively.

Table 1 lists the $(V–I)_0$ colors, heliocentric radial velocity and the measured equivalent widths of a few representative lines. Table 2 lists the stellar parameters adopted in the spectral synthesis analysis and the derived element abundances for all the program stars. An overall [α/Fe] abundance ratio, as the average of the single [Ca/Fe], [Si/Fe], [Mg/Fe] and [Ti/Fe] abundance ratios has also been computed.

Stellar temperatures are both estimated from colors and molecular lines, gravity from theoretical evolutionary tracks, according to the location of the stars on the Red Giant Branch (RGB), and adopting an average microturbulent velocity 2.0 km/s (see also Origlia et al. 1997). Equivalent widths are computed by Gaussian fitting the line profiles and the overall uncertainty is $\leq$10%.

Given the high reddening and crowding in the core region of these clusters, infrared photometry should be more suitable to infer reliable stellar temperatures and bolometric luminosities. Unfortunately, no J,H,K photometry of the brightest portion of the RGB in the central region of these clusters is currently available.

4.1. Terzan 4

In order to obtain a first guess estimate of the stellar temperatures, we use the existing V, I photometry of Ortolani, Barbuy, & Bica (1997), and we adopt their E(B-V)=2.35 and distance of 8.3 kpc. We also use the color-temperature transformation and bolometric corrections of Montegriffo et al. (1998), specifically calibrated for globular cluster giants. We find effective temperatures between 4750 and 5000 K, and $M_{bol} = -3.5$ to -4.0. Ortolani et al. (1997) also suggests an overall metallicity as low as [Fe/H]=–2.0. According to the empirical calibrations of the RGB features by Ferraro et al. (2000), at such a low metallicity the RGB Tip is expected to be located at $M_{bol} \approx -3.5$ and $T_{eff} \approx$4200 K, that is at a rather lower temperature than the one estimated by the $(V–I)_0$ reddening corrected color.

However, one has to take into account that Terzan 4 is a relatively low luminosity cluster with high degree of field contamination. The (V,V-I) CMD in the central region of Terzan 4 obtained by Ortolani, Barbuy, & Bica 1997 (see their Figure 4) and used to estimate the cluster reddening and distance is indeed very sparse and poorly populated. The barely defined RGB and HB sequences can be equally fitted with globular cluster mean ridge lines with quite different metallicities in the range $-2.0 \lesssim$ [Fe/H] $\lesssim -1.0$, by varying the reddening correction between $2.3 \lesssim \mathrm{E(B-V)} \lesssim 1.8$. Moreover, despite the very good seeing, by inspecting the V and I images and by computing Point Spread Function photometry (as also done by Ortolani, Barbuy, & Bica 1997) severe blending is still affecting the stars in the center, particularly star #2 and #3 in our sample, whose luminosities are very likely overestimated.

From our overall spectral analysis and in particular by simultaneously best-fitting the molecular line intensity and profiles we find much lower stellar temperatures of ≈3800-4000 K for the observed stars. By adopting these spectroscopic temperatures an overall [Fe/H]= −1.60 and a substantial α enhancement by a factor of ≈3 is obtained (see Table 2). We also measure a modest carbon depletion ([C/Fe]=–0.25±0.14 dex) and low (≤10) ^{12}C/^{13}C abundance ratios.

Fig. 2 shows our synthetic best fits superimposed on the observed spectra of the four giants in Terzan 4 in three major spectral regions of interest. Fig. 3 shows a small portion of the stellar spectra centered on the ^{12}CO(6,3) bandhead and on a couple of OH molecular lines around 1.62 μm, which are very sensitive to the stellar temperature. Superimposed on the observed spectra are two synthetic spectra at [Fe/H]=–1.60 adopting both the photometric and spectroscopic estimates of the stellar temperatures. The warmer spectra are too shallow to account for the observed molecular features since at temperatures significantly above 4000 K molecules barely survive.

The CO and in particular the OH molecular bands are indeed extremely sensitive thermometers in cool giants and make it possible to overcome most of the problems and uncertainties with photometric estimates of stellar temperatures in heavely reddened environments.

In order to check further the statistical significance of our best-fit solution, we compute synthetic spectra with $\Delta T_{\rm eff}= \pm 200$ K, Δlog g=±0.5 dex and $\Delta\xi= \mp 0.5$ km s^{-1}, and with corresponding simultaneous variations of ±0.2 dex of the C and O abundances to reproduce the depth of the molecular features. As a figure of merit we adopt the difference between the model and the observed spectrum (hereafter δ). In order to quantify systematic discrepancies, this parameter is more powerful than the classical χ^2 test, which is instead equally sensitive to *random* and *systematic* scatters (see also Origlia et al. 2003).

Since δ is expected to follow a Gaussian distribution, we compute $\overline{\delta}$ and the corresponding standard deviation for the best-fit solution and the *test models* with the stellar parameter and abundance variations quoted above. We then extract 10,000 random subsamples from each *test model* (assuming a Gaussian distribution) and we compute the probability P that a random realization of the data-points around a *test model* display a $\overline{\delta}$ that is compatible with the *best-fit* model. $P \simeq 1$ indicates that the model is a good representation of the observed spectrum.

The statistical test has been separately performed on portions of the spectrum mainly containing the CO bandheads or the OH lines. Fig. 4 shows the average results for the four stars measured in Terzan 4 with varying T_{eff}, log g and ξ, respectively. As can be appreciated our best fit solution gives in all cases a clear maximum in P (>99%) with respect to the *test models*. OH lines are very efficient in constraining the stellar temperature, while CO features are more sensitive to microturbulence: models with $\Delta T_{eff}= \pm 200$ K and $\Delta\xi= \pm 0.5$ km s^{-1}, respectively, are only significant at $> 1.5\sigma$ level. CO features and to somewhat less extent the OH lines are also sensitive to gravity: models with Δlog g$= \pm 0.5$ km s^{-1} lie at $\sigma \gtrsim 1$ from the best-fit solution.

The cooler stellar temperatures inferred by our spectral analysis, which are also in better agreement with the empirical calibrations of the tip RGB temperatures by Ferraro et al. (2000), require a somewhat lower reddening correction, namely E(B–V)$\leq$2.0, but near infrared photometry would be most valuable to measure better the true reddening and distance of this cluster.

Given the large uncertainty affecting the photometric estimate of the stellar temperatures in this cluster and as a further check of the reliability of our overall spectral analysis, we also perform the following experiment. Acceptable fits to the observed H-band spectra have been computed by adopting different temperatures in the range $3800 \leq T_{eff} \leq 5000$. The corresponding range in variation of the iron abundance turns out to be rather small, between ≈–1.6 and –1.4, while more dramatic variations of the carbon and oxygen abundances have to be adopted. Figure 5 shows the average [O/Fe] and [C/Fe] abundance ratios required to fit the observed spectra. For temperatures above ≈4500 K, [C/Fe] exceeds the solar value, while normally in RGB stars it is somewhat depleted due to the first dredge-up. More dramatic, for temperatures above ≈4200 K, [O/Fe] abundance ratios exceeding 10 times the solar value and up to ≈150 at $T_{eff} \approx 5000$ K are needed to fit the relatively deep OH features in the observed spectra (see Figure 3). This is definitely unlikely. Also, large oxygen abunandances are fully inconsistent with the presence of a blue HB, as inferred from the CMD, typical of metal poor clusters (see also Ortolani et al. 2001).

4.2. Terzan 5

We use the V,I photometry of Ortolani, Barbuy & Bica (1996), the distance estimate of 5.6 kpc and E(B–V)=2.39 (Barbuy et al. 1998) and the color-temperature transformation of Montegriffo et al. (1998) to infer temperatures ranging from 3800 to 4000 K for our four observed giants (cf. Table 1). More recently, Cohn et al. (2002) by means of HST NICMOS photometry inferred a slightly lower E(B-V)=2.16 reddening correction, which implies slightly lower (by ≈200 K) stellar temperatures, in better agreement with the spectroscopic temperatures as inferred from the OH lines and reported in Table 2.

According to its RGB morphology (see also Ortolani et al. 2001), which shows a strong curvature in the optical CMD, Terzan 5 should be extremely metal rich, close to Solar. In such a high metallicity regime cool giants near the tip of the RGB suffer dramatic molecular blanketing

effects in the V,I photometric bands, making it impossible to estimate reliable BC_V and BC_I bolometric corrections.

Best-fitting solutions to the observed spectra of the four giants in Terzan 5 (see Fig. 6) give an overall [Fe/H]≈ -0.2 dex, an [α/Fe] enhancement by $\approx$+0.3 dex and a [C/Fe] depletion -0.32 ± 0.18 dex (see Table 2). A low $^{12}C/^{13}C \leq 10$ isotopic abundance ratio has been also measured in this metal rich cluster.

In order to check further the robustness of our best-fit solution, the same statistical test done for Terzan 4 has been repeated here. Fig. 7 shows the average results of the four stars measured in Terzan 5 for the CO and OH features with varying T_{eff}, log g and ξ, respectively. Our best fit solution provides in all cases a clear maximum in P (>97%) with respect to the *test models*. Models with $\Delta T_{eff} = \pm 200$ K and $\Delta\xi = \pm 0.5$ km s^{-1}, respectively, are only significant at $> 2\sigma$ level, while models with Δlog g$= \pm 0.5$ km s^{-1} are still significant at $\approx 1\sigma$ level.

Two additional stars (#5 and #6 according to our numbering, or equivalently #2189 and #363, respectively, according to the nomenclature of Ortolani et al. 1996, see also Table 3) have been observed in Terzan 5. These stars have photospheric parameters similar to stars #3 and #4 but slightly lower abundances (by $\approx$0.1 dex). However, the cluster membership of these additional stars is doubtful since they show heliocentric radial velocities of –69 and –47 km s^{-1}, respectively, significantly lower (by $\approx$24 and 46 km s^{-1}) than the average cluster value (see Sect. 4). These stars may plausibly be M giant members of the bulge field population.

5. Discussion and Conclusions

Our high resolution spectroscopy confirms the photometric metallicities of Terzan 4 and Terzan 5 as obtained from the morphology of the RGB (Ortolani et al. 2001). These two bulge globular clusters were thought to lie at the extremes of the bulge abundance distribution; our detailed abundance analysis indicates that this is indeed the case. Our findings strengthen the analogy between the properties of the bulge globular clusters and the stellar field population in the bulge and remain consistent with a common formation history.

In addition, the detailed study of the abundance patterns indicates oxygen and other $\alpha-$element enhancement at the level of $\approx +0.5$ dex in the metal–poor cluster, typical of the halo population, and of $\approx +0.3$ dex in the metal rich one. The enhanced $\alpha-$element abundances for Terzan 5 are noteworthy, as enhanced alphas at Solar metallicity is a hallmark of bulge stars, reinforcing the scenario of a rapid enrichment of the bulge, similar to the halo but possibly requiring a higher rate of star formation (see e.g. Matteucci, Romano & Molaro 1999; Wyse 2000).

The direct measurement of the $^{12}C/^{13}C$ abundance ratio provides major clues to the efficiency of the mixing processes in the stellar interiors during the evolution along the RGB. Both the metal-poor and metal-rich giants in the bulge clusters show very low $^{12}C/^{13}C \leq 10$ ratios. The classical

theory (Iben 1967; Charbonnel 1994 and reference therein) predicts a decrease of $^{12}C/^{13}C \approx 40$ after the first dredge–up, the exact amount mainly depending on the chemical composition and the extent of the convective zone. However, much lower $^{12}C/^{13}C \leq 10$ values have been measured in several metal-poor halo giants both in the field and in globular clusters (see e.g. Suntzeff & Smith 1991, Shetrone 1996, Gratton et al. 2000 and references therein). Also the bright giants of ω Centauri show very low $^{12}C/^{13}C \leq 7$ over the whole metallicity range spanned by the multiple stellar population in the cluster (see Brown & Wallerstein 1993; Zucker, Wallerstein & Brown 1996; Wallerstein & Gonzalez 1996; Vanture, Wallerstein & Suntzeff 2002; Smith et al. 2002), including the most metal-rich RGB stars (see Origlia et al. 2003). Additional mixing mechanisms due to further *cool bottom processing* (see e.g. Charbonnel 1995; Denissenkov & Weiss 1996; Cavallo, Sweigart & Bell 1998; Boothroyd & Sackmann 1999; Weiss, Denissenkov & Charbonnel 2000) are thus a common feature during the evolution along the RGB, regardless the stellar metallicity and environment.

LO acknowledges the financial support by the Agenzia Spaziale Italiana (ASI) and the Ministero dell'Istruzione, Università e Ricerca (MIUR). RMR acknowledges support from grant number AST-0098739, from the National Science Foundation. The authors are grateful to the staff at the Keck observatory and to Ian McLean and the NIRSPEC team. The authors wish to recognize and acknowledge the very significant cultural role and reverence that the summit of Mauna Kea has always had within the indigenous Hawaiian community. We are most fortunate to have the opportunity to conduct observations from this mountain.

REFERENCES

Armandroff, T. E., & Zinn, R. 1988, AJ, 96, 588

Barbuy, B., Castro, S., Ortolani, S., & Bica, E. 1992, A&A, 259, 607

Barbuy, B., Bica, E., & Ortolani, S. 1998, A&A, 333, 117

Bièmont, E., & Grevesse, N. 1973, *Atomic Data and Nuclear Data Tables*, 12, 221

Boesgaard A.M., King J.B., Deliyannis C.P., Vogt S. 1999, AJ, 117, 492

Boothroyd, A. I., & Sackmann, I. J. 1999, 1999, ApJ, 510, 232

Brown, J, & Wallerstein, G. 1993, AJ, 106, 133

Carney, B. W. 1996, PASP, 108, 877

Carretta, E., Cohen, J., Gratton, R.G., & Behr, B. 2001, AJ, 122, 1469

Carretta, E., Gratton, R.G., & Sneden, C. 20001, A&A, 356, 238

Cavallo, R. M., Sweigart, A. V., & Bell, R. A. 1998, ApJ, 492, 575

Charbonnel, C. 1994, A&A, 282, 811

Charbonnel, C. 1995, ApJ, 453, L41

Cohn, H. N., Lugger, P.M., Grindlay, J.E., & Edmonds, P.D. 2002, ApJ, 571, 818

Cohen, J. G., Gratton, R. G., Behr, B. B., & Carretta, E. 1999, ApJ, 523, 739

Denissenkov, P. A, & Weiss, A. 1996, A&A, 308, 773

Ferraro, F.R., Montegriffo, P., Origlia, L. & Fusi Pecci, F. 2000, AJ, 119, 1282

Gratton, R., Sneden, C., Carretta, E., & Bragaglia, A. 2000, A&A, 354, 169

Grevesse, N., & Sauval, A. J. 1999, *Space Science Reviews*, 85, 161

Harris, W. E. 1996, AJ, 112, 1487

Harris, W.E. 1999, http://www.physics.mcmaster.ca/Globular.html

Iben, I. J. 1967, ApJ, 147, 642

Johnson, H. R., Bernat, A. P., & Krupp, B. M. 1980, ApJS, 42, 501

Kraft, R. P. 1994, PASP, 106, 553

Lambert, D. L., Brown, J. A., Hinkle, K. H., & Johnson, H. R. 1984,

ApJ, 284, 223

Matteucci, F., Romano, D., & Molaro, P. 1999, A&A, 341, 458

McLean, I. et al. 1998, SPIE, 3354, 566

McWilliam, A., & Rich, R.M. 1994, ApJS, 91, 749

McWilliam, A. 1997, ARA&A, 35, 503

Meléndez, J., & Barbuy, B. 1999, ApJS, 124, 527 (MB99)

Minniti, D. 1995, A&AS, 113, 299

Montegriffo, P., Ferraro, F.R., Fusi Pecci, F., & Origlia, L., 1995, MNRAS, 276, 739

Origlia, L., Moorwood, A. F. M., & Oliva, E. 1993, A&A, 280, 536

Origlia, L., Ferraro, F. R., Fusi Pecci, F., & Oliva, E. 1997, A&A, 321, 859

Origlia, L., Rich, R. M., & Castro, S. 2002, AJ, 123, 1559 (ORC02)

Origlia, L., Ferraro, F. R., Bellazzini, M. & Pancino, E. 2003, ApJ, 591, 916

Ortolani, S., Barbuy, B., & Bica, E. 1996, A&A, 308, 733

Ortolani, S., Barbuy, B., & Bica, E. 1997, A&A, 319, 850

Ortolani, S., Barbuy, B., & Bica, E., A. Renzini, M. Zoccali, R. M. Rich, & Cassisi, S. 2001, A&A, 376, 878

Rich, R.M., & McWilliam, A. 2000, SPIE, 4005, 150

Smith, V. V., & Lambert, D. L. 1985, ApJ, 294, 326

Smith, V. V., & Lambert, D. L. 1990, ApJS, 72, 387

Smith V. V., Terndrup, D. M., & Suntzeff, N. B. 2002, ApJ, 579, 832

Suntzeff, N. B., & Smith, V. V. 1991, ApJ, 381, 160

Vanture, A. D., Wallerstein, G., & Suntzeff, N. B. 2002, ApJ, 569, 984

Wallerstein, G., & Gonzalez, G. 1996, MNRAS, 282, 1236

Weiss, A., Denissenkov, P. A., & Charbonnel, C. 2000, A&A, 356, 181

Wheeler, J.C., Sneden, C., & Truran, J.W. 1989, ARA&A, 27, 279

Wyse, R. F. G. 2000, Ap&SS, 267, 145

Zucker, D., Wallerstein, G., & Brown, J. 1996, PASP, 108, 911

Table 1. $(V–I)_0$ colors, heliocentric radial velocity and equivalent widths (mÅ) of some representative lines for the observed stars in Terzan 4 and Terzan 5.

	Terzan 4				Terzan 5					
star	#1	#2	#3	#4	#1	#2	#3	#4	#5	#6
ref #[a]	471	510	456	464	1614	2167	3235	401	2189	363
$(V–I)_0^b$	1.55	1.49	1.34	1.42	1.81	1.81	1.97	2.10	2.15	2.52
v_r [km s^{-1}]	–55	–54	–45	–45	–88	–94	–95	–96	–69	–47
Ca λ1.61508	49	60	26	30	208	262	287	297	212	234
Fe λ1.61532	73	72	57	57	229	254	270	262	249	249
Fe λ1.55317	51	57	50	50	215	223	213	200	178	187
Mg λ1.57658	–	–	–	–	445	447	437	438	–	428
Mg λ1.59546	49	55	50	44	–	–	–	–	188	–
Si λ1.58884	386	416	361	377	505	518	534	530	481	495
OH λ1.55688	106	212	87	106	307	334	355	358	347	344
OH λ1.55721	100	217	78	109	295	338	365	367	357	355
Ti λ1.55437	236	246	196	196	404	443	450	429	421	413

Note. —

[a] Stars in Terzan 4 from Ortolani et al. (1997), in Terzan 5 from Ortolani et al. (1996).

[b] Reddening corrected colors adopting E(B-V)=2.0 for Terzan 4 and E(B-V)=2.16 for Terzan 5 (see Sect. 4).

Table 2. Adopted stellar atmosphere parameters and abundance estimates.

	Terzan 4				Terzan 5					
star	#1	#2	#3	#4	#1	#2	#3	#4	#5	#6
$T_{\rm eff}^{a}$ [K]	3800	3800	4000	4000	4000	3800	3600	3600	3600	3600
log g	0.5	0.5	1.0	1.0	1.0	0.5	0.5	0.5	0.5	0.5
ξ [km s^{-1}]	2.0	2.0	2.0	2.0	2.0	2.0	2.0	2.0	2.0	2.0
[Fe/H]	–1.60	–1.58	–1.64	–1.60	–0.22	–0.19	–0.23	–0.20	–0.33	–0.30
	±.10	±.10	±.11	±.11	±.09	±.10	±.07	±.10	±.08	±.09
[O/Fe]	+0.40	+0.60	+0.55	+0.62	+0.31	+0.30	+0.28	+0.25	+0.29	+0.26
	±.11	±.11	±.13	±.13	±.11	±.11	±.11	±.12	±.11	±.12
[Ca/Fe]	+0.53	+0.58	+0.54	+0.50	+0.32	+0.29	+0.33	+0.30	+0.33	+0.30
	±.16	±.18	±.19	±.19	±.14	±.12	±.11	±.13	±.12	±.12
[Si/Fe]	+0.57	+0.55	+0.59	+0.50	+0.37	+0.29	+0.33	+0.40	+0.38	+0.30
	±.15	±.15	±.17	±.19	±.18	±.18	±.17	±.18	±.15	±.15
[Mg/Fe]	+0.39	+0.43	+0.42	+0.40	+0.32	+0.22	+0.28	+0.30	+0.38	+0.30
	±.18	±.19	±.19	±.19	±.15	±.15	±.14	±.16	±.17	±.18
[Ti/Fe]	+0.40	+0.47	+0.44	+0.44	+0.37	+0.34	+0.35	+0.25	+0.33	+0.20
	±.19	±.19	±.19	±.18	±.14	±.14	±.14	±.15	±.13	±.14
[α/Fe][a]	+0.47	+0.51	+0.50	+0.46	+0.34	+0.28	+0.32	+0.31	+0.35	+0.27
	±.13	±.13	±.14	±.14	±.12	±.12	±.10	±.12	±.10	±.11
[C/Fe]	–0.40	–0.22	–0.06	–0.30	–0.48	–0.31	–0.07	–0.40	–0.47	–0.30
	±.08	±.05	±.06	±.05	±.05	±.07	±.05	±.04	±.06	±.05

Note. —

[a] [α/Fe] is the average [$< {\rm Ca, Si, Mg, Ti} >$ /Fe] abundance ratio (see Sect. 4).

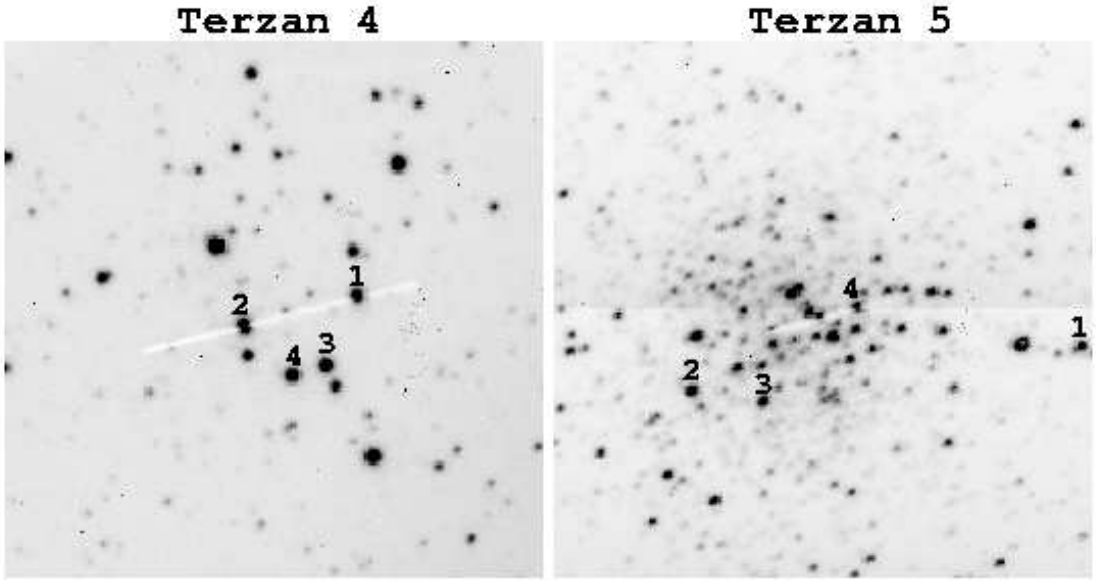

Fig. 1.— H band images of the core regions of Terzan 4 and Terzan 5 as imaged by the slit viewing camera (SCAM) of NIRSPEC. The field of view is 46″on a side and the image scale is 0.″183 $pixel^{-1}$; the slit is 12″ long the observed stars are numbered (cf. Table 1 and 3).

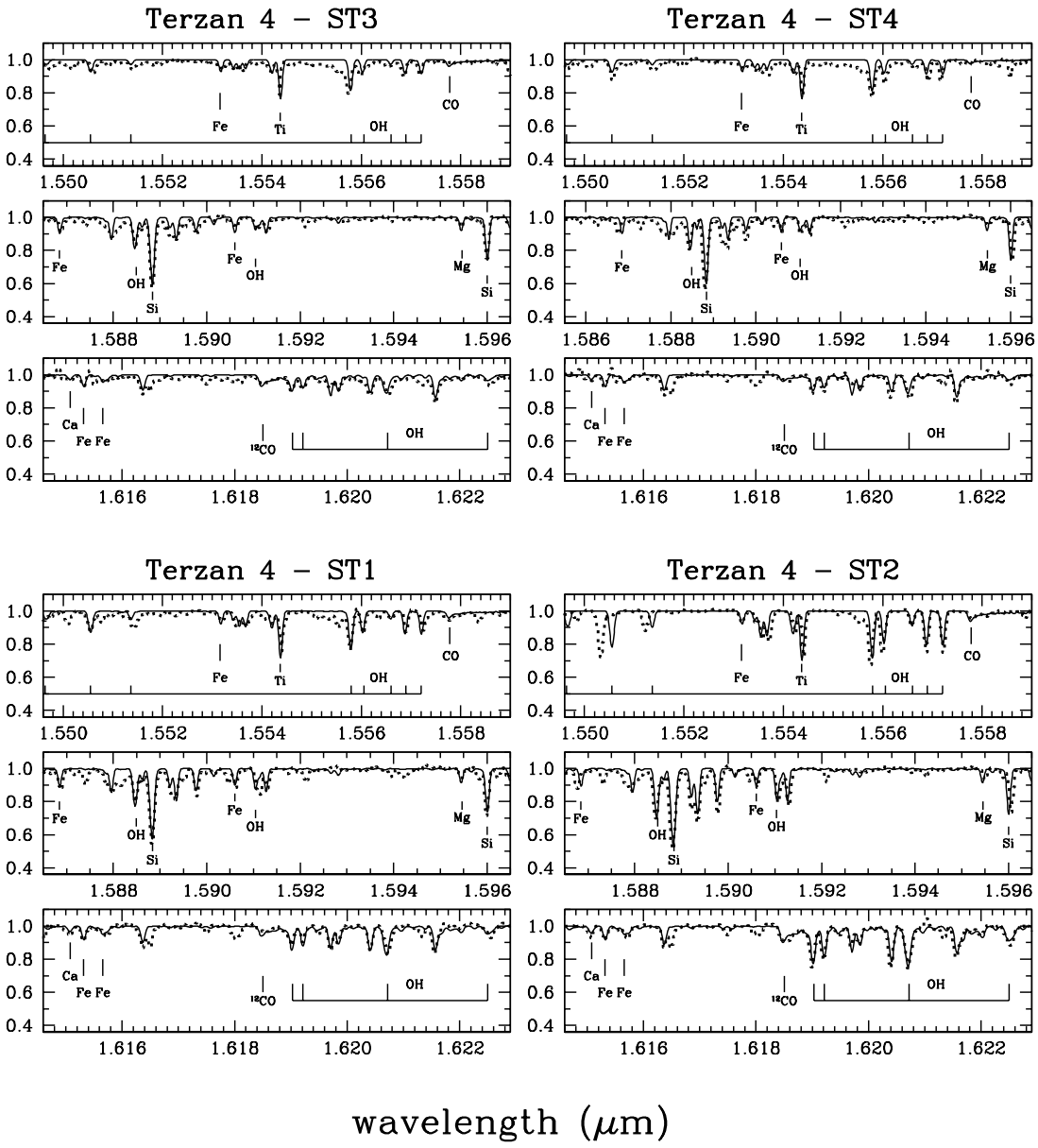

Fig. 2.— Selected portions of the observed echelle spectra (dotted lines) of the four giants in Terzan 4 with our best fit synthetic spectrum (solid line) superimposed. A few important molecular and atomic lines of interest are marked.

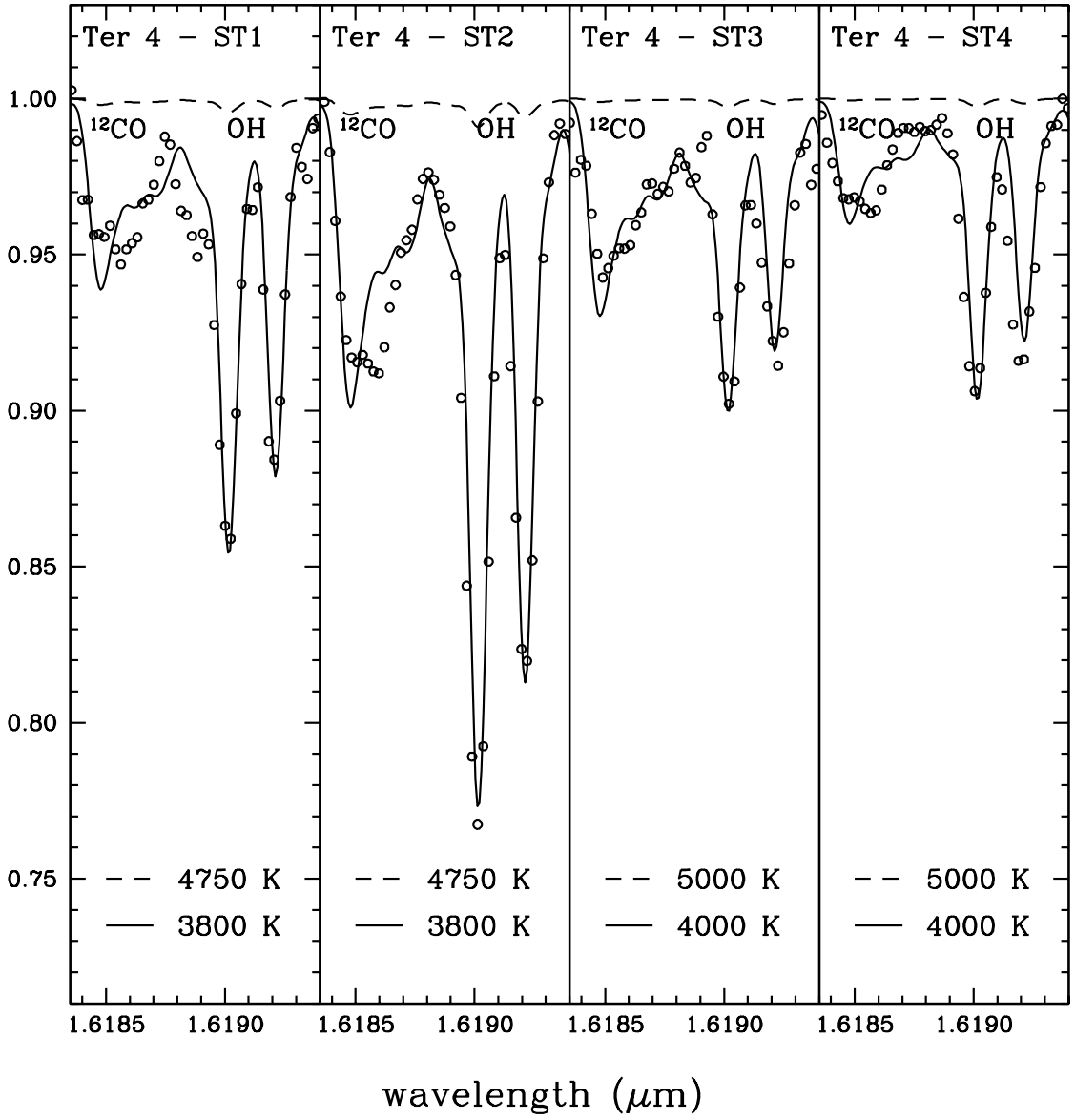

Fig. 3.— Observed spectra (dotted lines) centered on the ^{12}CO(6,3) bandhead and on two OH molecular lines around 1.62 μm of the four giants in Terzan 4. Superimposed are two synthetic spectra at [Fe/H]=–1.6 and adopting the two different stellar temperatures (dashed and full lines) reported in the bottom end of each panel (see also Sect. 4).

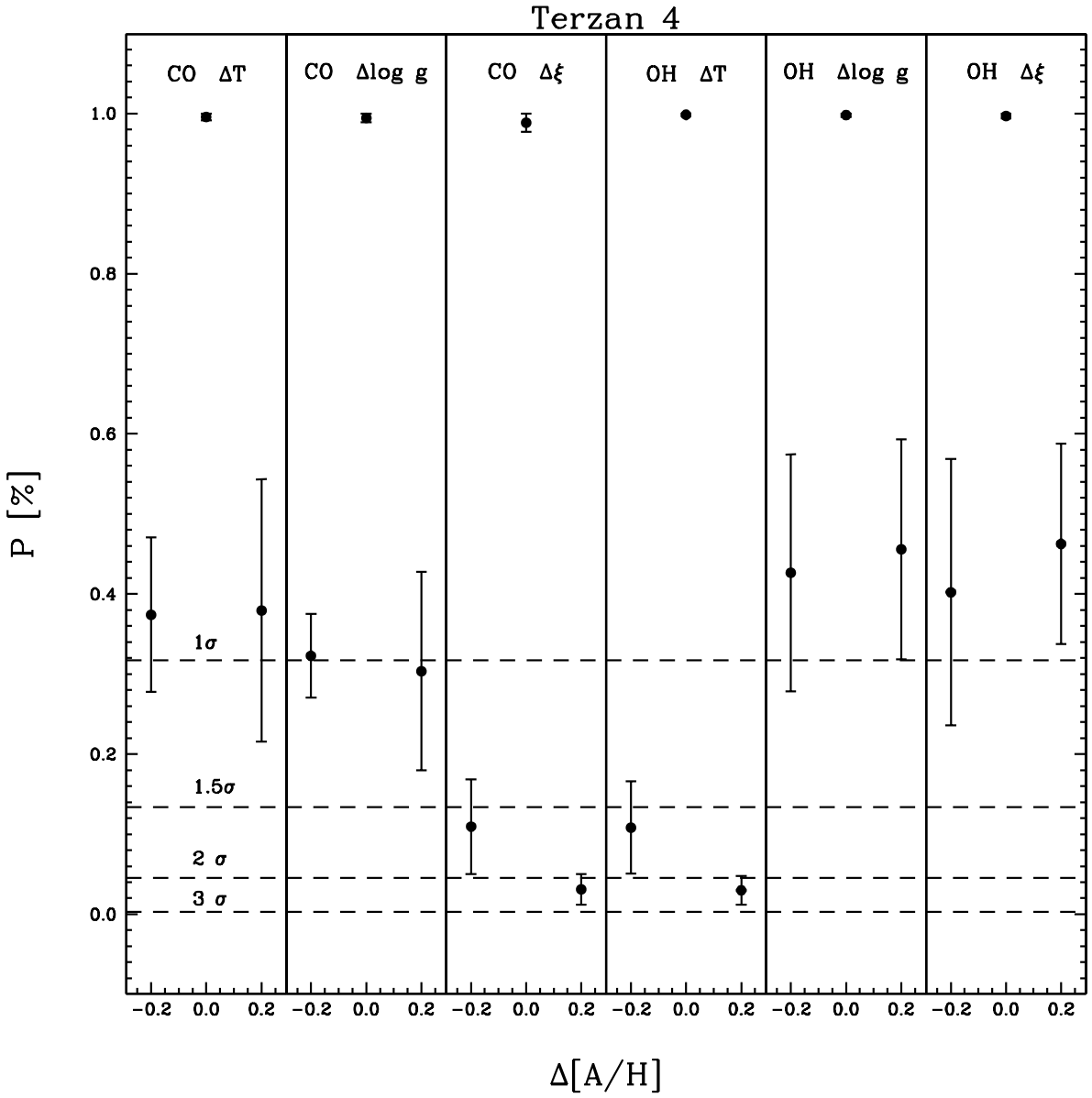

Fig. 4.— Average probability of a Monte Carlo realization for the best fit solution for the four stars in Terzan 4 (see text). This figure shows that our best fit model is stable with respect to variations in the stellar parameters. The x-axis is The best fit is compared with $\Delta[A/H]$ of ± 0.2 with respect to the best-fit to compensate for a $\Delta T_{\rm eff}= \pm 200$ K, Δlog g$=\pm 0.5$ dex and $\Delta\xi= \pm 0.5$ km s^{-1} variations, respectively. Starting from the left, the first three panels show the results for the the CO band-heads, the other three panels for the OH features. Dashed lines indicate 1, 1.5, 2 and 3σ probabilities.

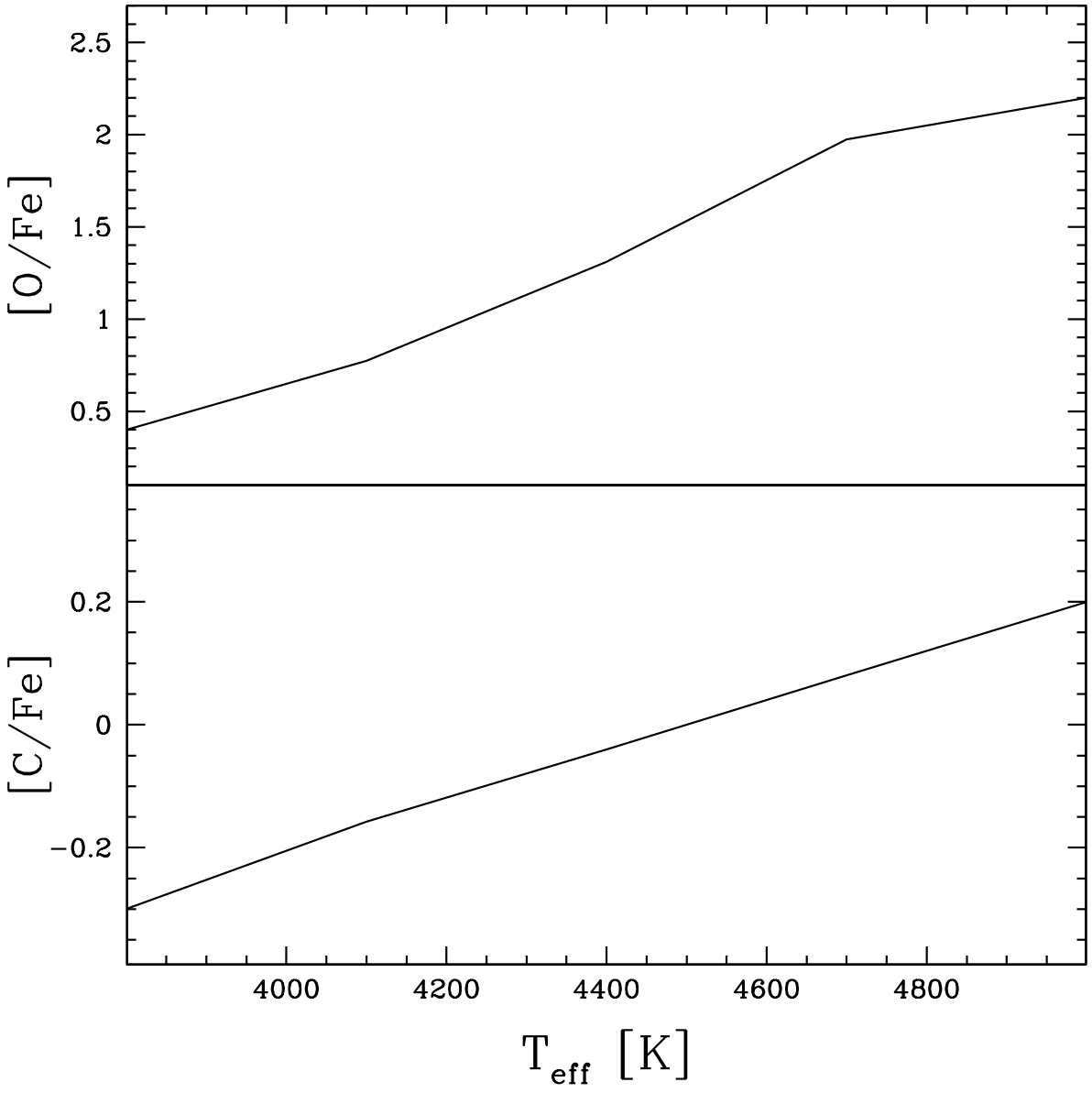

Fig. 5.— Average [C/Fe] (lower panel) and [O/Fe] (upper panel) abundance ratios as inferred by adopting different stellar temperatures for the four giant stars in Terzan 4 (see also Sect. 4). Notice that adopting temperatures in excess of 4000K leads to estimates of [O/Fe] that are unreasonable.

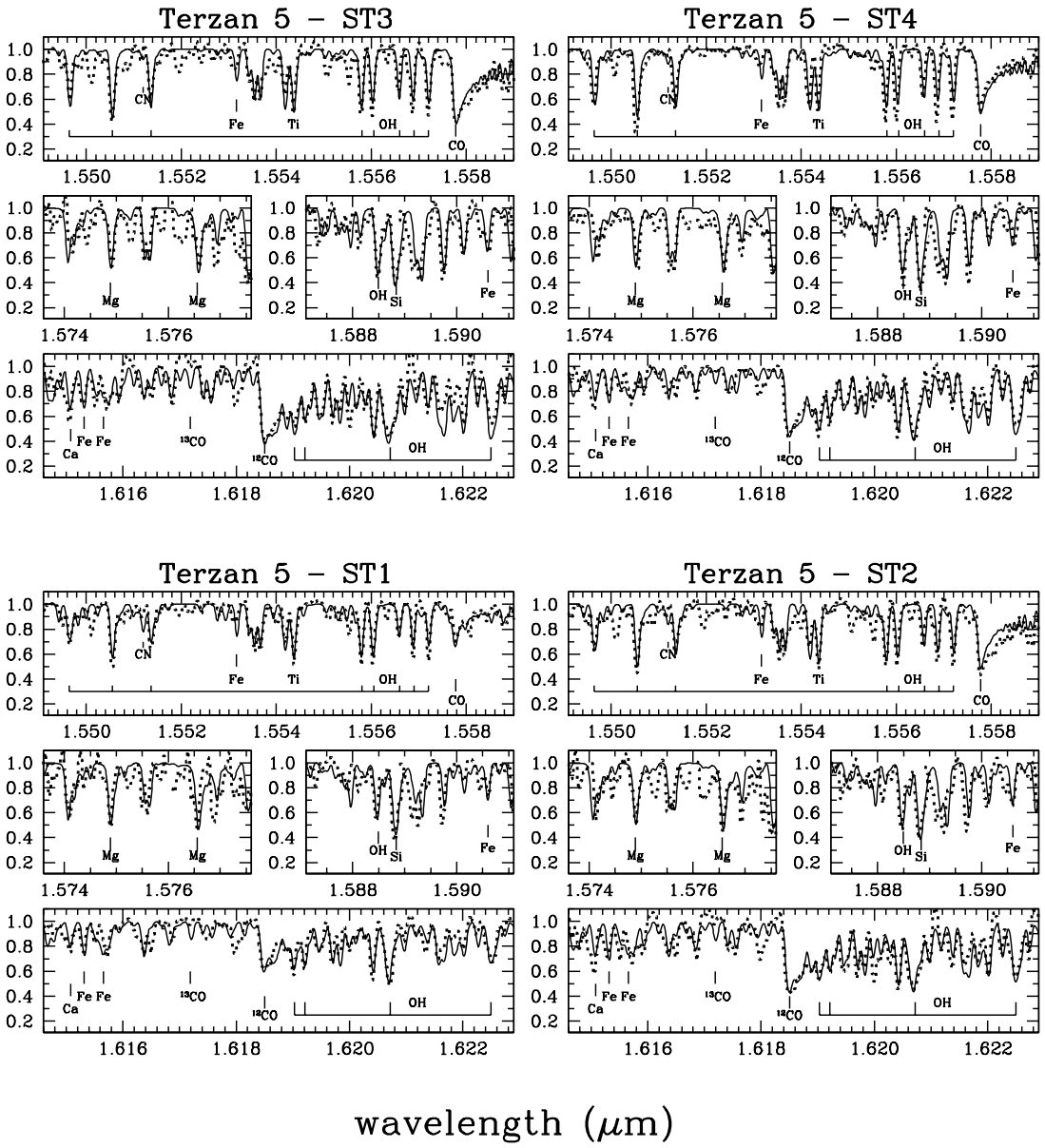

Fig. 6.— As in Fig. 2 but for the four giant stars in Terzan 5.

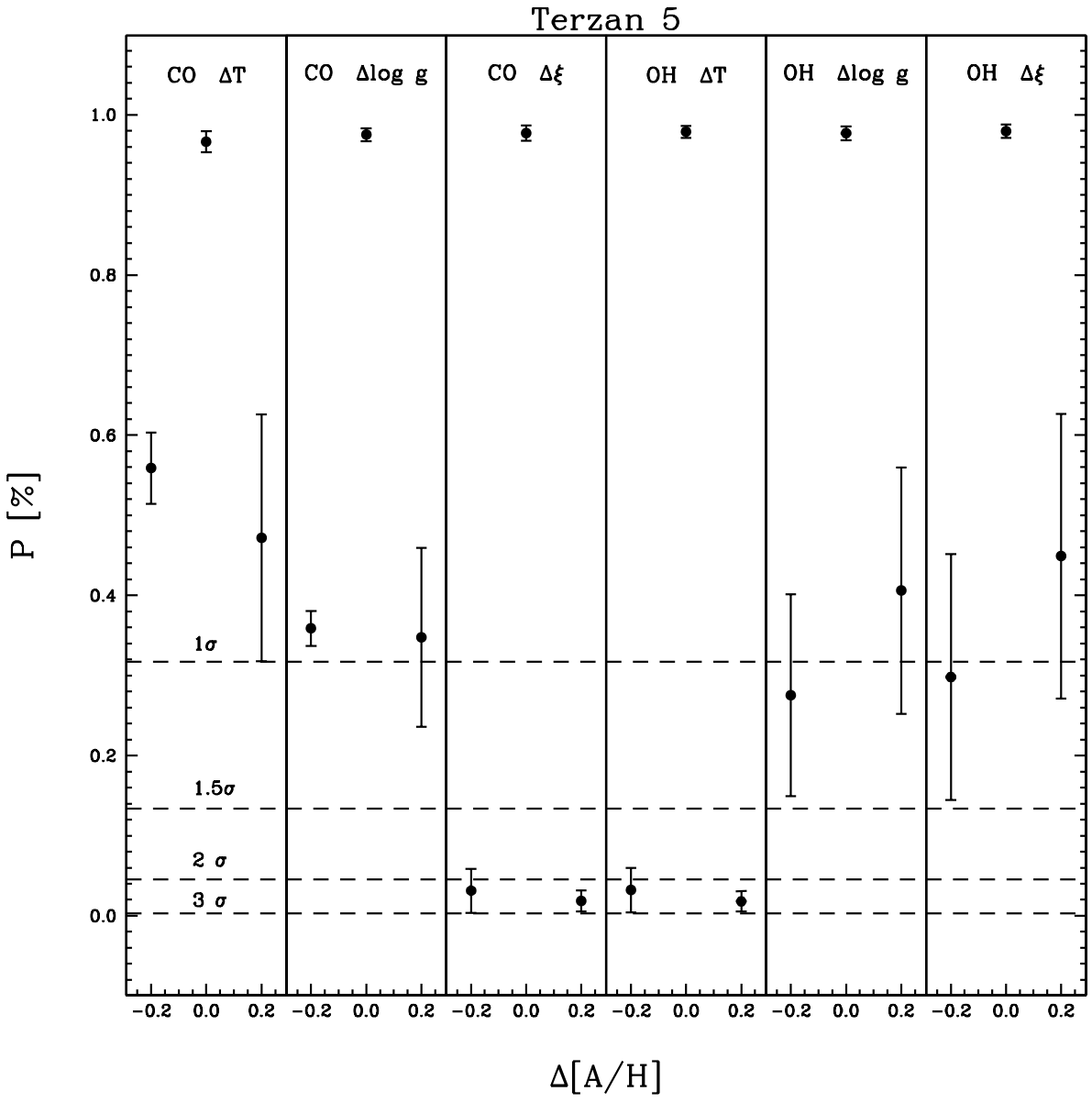

Fig. 7.— As in Fig. 4 but for Terzan 5.